Exploring LIGO Sensitivity Across Binary Black Hole Parameter Space

LIGO SURF 2022 Final Report
LIGO Technical Note T2200251

Daniela Hikari Yano[1],
Mentors: Rhiannon Udall[2], Jacob Golomb[2] and Alan Weinstein[2]

[1]Barnard College
[2]California Institute of Technology, LIGO Laboratory

Oct 19th, 2022

Abstract

As we look ahead to LIGO, Virgo and KAGRA (LVK)'s next observational run (O4) and future gravitational wave observatories such as Cosmic Explorer, understanding the sensitivity of a detector network to compact binary coalescences (CBCs) is important for estimating the merger rate density. The parameter space of CBCs is composed of many parameters, which are used to characterize the binary systems. In this work, we explore how the network sensitivity (space-time sensitive hypervolume) changes according to changes in the CBC population parameter space. Using Monte Carlo simulations, we calculate the averaged space-time sensitive hypervolume for different parameter configurations, marginalizing over subsets of the parameter space so that we can compare them.

1 Introduction

1.1 Gravitational Waves (GW)

Gravitational Waves are ripples of space-time caused by massive accelerating objects. When two Black Holes or Neutron Stars orbit each other, they radiate energy in form of GWs until they merge. In 2015, LIGO made its first direct detection of gravitational waves, GW150914 [1]. Since then GW signals from mergers of Binary black holes (BBHs) and Neutron stars (NSs) have been detected. The third LVK Collaboration Gravitational-Wave Transient Catalog (GWTC-3) contains 90 GW signals from CBCs observed thorugh the first three observing runs of LIGO-Virgo [2].

The space-time distortions caused by gravitational waves are transverse to direction of propagation. Each LIGO detector is a Michelson interferometer with 4km arms. Each arm has a Fabry-Perot resonant cavity that allows to measure the change in the length of the arms [3]. This difference is used to calculate the strain, which is defined as

$$h = \Delta L/L. \tag{1}$$

The strain (h) can also be described as:

$$h = h_+ F_+ + h_\times F_\times \tag{2}$$

where plus and cross represents the polarizations, and F_+ and $F_\times$ represent the detector antenna response as a function of the right ascension, declination, and polarization angle of the source.

1.2 Overview of the study

The current LIGO [3], Virgo [4] and KAGRA [5] (LVK) network can not possibly detect all the compact binary coalescences (CBCs) in the Universe, but the next generation of detectors, as Cosmic Explorer (CE), will have sensitivity to a much larger fraction of CBCs in the Universe. Therefore, it is important to understand how sensitive the LVK network is for those mergers, both in the present time, as well as make estimates for the future. The CBCs can be characterized by their source parameters, which are divided into intrinsic parameters: masses (m_1, m_2) and spins $(S_{x1}, S_{y1}, S_{z1}, S_{x2}, S_{y2}, S_{z2})$, and extrinsic parameters: right ascension (α), declination (δ), luminosity distance (d_L), inclination (θ_{JN}), polarization angle $(\psi])$, time of coalescence (t_c), and phase at coalescence (ϕ_c) [6].
This work uses the space-time sensitive hypervolume $\langle VT \rangle$ as the metric to understand the sensitivity of the LVK network. The goal of this study is to understand how the $\langle VT \rangle$ changes according to changes in the parameter space population of CBCs and the resulting waveform properties. The merger rate density can be estimated from the space-time sensitive hypervolume and the the number of detected signals obtained from LVK's observational runs. Therefore, understanding the detector network sensitivity to Gravitational Waves (GW) from CBCs will lead to more information about the cosmic population.
This project will use available computational tools such as PyCBC[7] and Bilby [8] to generate CBC populations and the waveforms produced from the mergers. By using Monte Carlo simulations, it will calculate the dependence of the space-time sensitive hypervolume on selected parameters. The probability of detections are determined using the predicted network signal-to-noise ratio (SNR) of the injected signal.

1.3 Signal-to-noise ratio (SNR)

The general noise-weighted inner product is used to determine the probability of detection of a signal from a CBC. The SNR is calculated using the inner product:

$$\langle a|b\rangle = 4\int_{f_{min}}^{f_{max}} \frac{\tilde{a}^*(f)\tilde{b}(f)}{S_n(f)} df \tag{3}$$

where S_n is the Power spectral density (PSD) of each detector. The SNR (ρ) is defined as:

$$\rho = \frac{\langle d|h\rangle}{\sqrt{\langle h|h\rangle}} \tag{4}$$

where

$$d = h' + n \tag{5}$$

where h' is the injected waveform and n is the noise. In special, we are mostly interested in the optimal SNR, defined as:

$$\rho^2_{opt} = \langle h|h\rangle \tag{6}$$

For ρ_{opt}, the same waveform is used for injection and recovery. The optimal SNR assumes that the template waveform h is exactly equal to the signal in the data h' (up to an overall multiplicative scale). In Section 3, we are going to conduct one study using a different injected and recovery waveform, for which we are going to use Eq. 3. The SNR is calculated for each detector, and the optimal network SNR can be calculated as the square root of each individual SNR squared:

$$\rho^2 = \sum_{network} \rho_i^2 \tag{7}$$

The probability of the detection is determined by the SNR, and we designate anything above our threshold of 10 as detected.

1.4 Merger rate density

Estimating the merger rate density is important to understanding the cosmic population. The mean number of detected signals of astrophysical origin Λ_1 above the chosen threshold, is related

to $\hat{R}$, the rate density (events per unit time per comoving volume) of binary coalescenses, by [9]:

$$\hat{R} = \frac{\Lambda_1}{\langle VT \rangle} \tag{8}$$

where $\langle VT \rangle$ is the averaged space-time sensitive hypervolume.

1.5 Space-time sensitive hypervolume $\langle VT \rangle$

The $\langle VT \rangle$ is the metric used to define how well the detectors can observe a given configuration of CBCs, and is the main topic of this study. The $\langle VT \rangle$ is defined as:

$$\begin{aligned} \langle VT \rangle &= \int \frac{dV_c}{dz} \frac{dt_{src}}{dt_\oplus} dt_\oplus dz \int \pi(\theta) p_{det}(\theta, z) d\theta \\ &= V_0 \int \pi(z) dt_\oplus dz \int \pi(\theta) p_{det}(\theta, z) d\theta \\ &\approx \frac{V_0 T}{N} \sum_{k \sim \pi(\theta,z)}^{N} p_{det}(k) \end{aligned} \tag{9}$$

where t_{src} is the source time, $t_\oplus$ is the detector time, z is the redshift, and V_c is the comoving volume. The V_0 is the factor that takes into account the cosmological effects. The integral is transformed in a sum in the last line, so that we can do a Monte Carlo simulation. We are sampling over the probability distribution of the parameters, θ represents the intrinsic and extrinsic parameters, excluding the luminosity distance (d_l), and p_{det} is the probability of detection of the signal, based on the SNR.

2 Methodology

To carry out the Monte Carlo integration it is necessary to generate populations of CBCs waveforms ($\pi(\theta, z)$) to numerically solve for the space-time sensitive hypervolume. Those populations can be fixed over some parameter, for example, populations where all the Binary Black Holes have the same mass, or they can be over some distribution.

2.1 Generating BBH mergers waveforms

To generate waveforms, this project uses PyCBC waveform model families [7]. Specifically, IMRPhenomXP and IMRPhenomXPHM[10, 11] which is a model in the frequency-domain for the gravitational-wave signal in the precessing frame, to simulate the merger of BBHs.

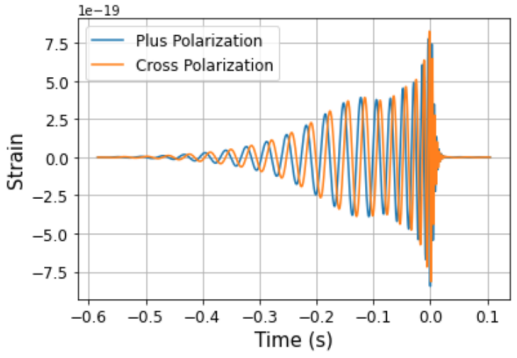

Figure 1. *An example of a simulated waveform in time domain. The waveform was generated for black holes of 35 $M_\odot$, at a distance of 1 Mpc, using the IMRPhenomXP approximant. The waveform is tapered to zero at frequencies below 20 Hz because of computational costs.*

PyCBC has methods that generate waveforms in the time and frequency domains. The methods to generate those waveforms receives as input an waveform model, and the following parameters: masses, spins, inclination, phase at coalescence, and luminosity distance. The methods will return the components of Eq. 2, allowing for the calculation of the strain.

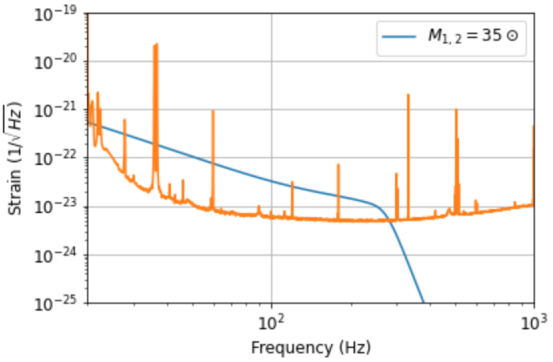

Figure 2. *An example of a simulated waveform in frequency domain. The blue line is the waveform simulated for a black hole merger of equal masses ($m_1 = m_2 = 35M_\odot$), at a distance of 1 Mpc. The orange line is the noise of the detector for O3 in the Hanford detector.*

2.2 Generating populations

In this project, the generation of the CBC population ($\pi(\theta, z)$) is carried in three steps, which are designed to speed up the generation of the waveform population. In each of those steps, the parameters are generated according to probability distributions, using Bilby priors[12, 8]. The first step is drawing the parameters necessary to generate the waveforms: masses (m_1, m_2), spins components $(S_{x1}, S_{y1}, S_{z1}, S_{x2}, S_{y2}, S_{z2})$, inclination (θ_{JN}), and phase at coalescence (ϕ_c). For each of those configurations, the waveforms are generated at a fixed luminosity distance (d_L) of 1 Mpc.

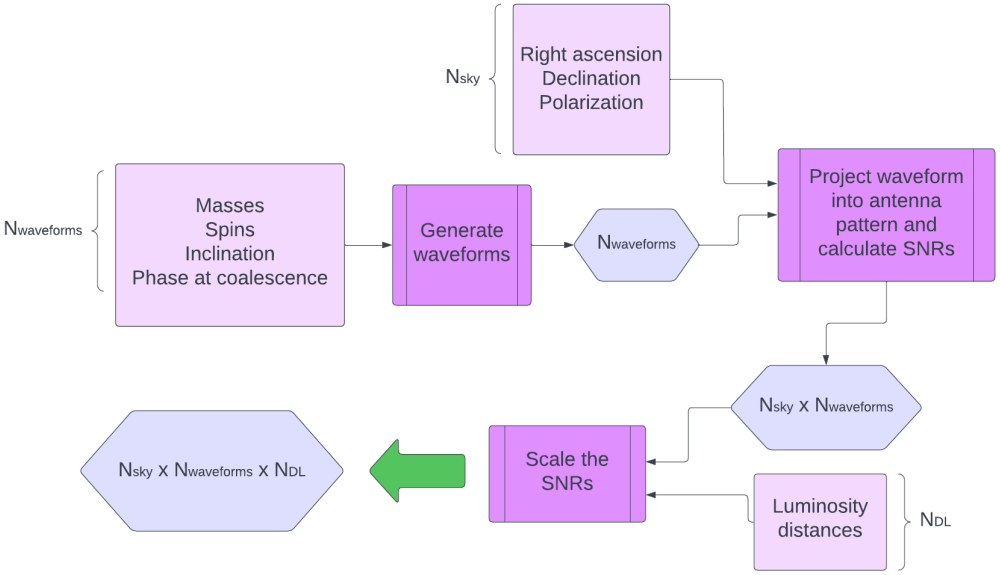

Figure 3. *Flowchart showing the pipeline used by SIFCE [13] to generate a population and calculate SNRs.*

The second step is drawing the sky parameters (right ascension (α), declination (δ), and polarization (ψ) from the prior probability distribution. The sky parameters are used to calculate the detector antenna response, as shown in Eq. 2. For each waveform generated in the first step, a N number of sky configurations are drawn, and the corresponding SNR is calculated.

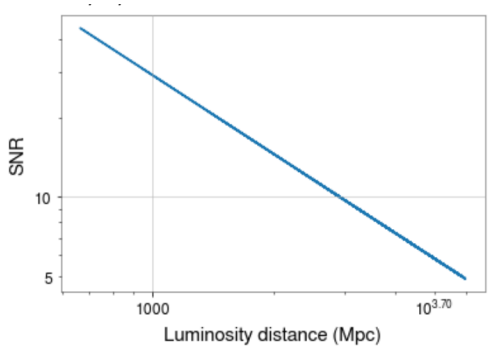

Figure 4. *SNR for 100 binary black hole mergers of equal masses ($m_1 = m_2 = 35M_\odot$), for different luminosity distances, in logarithm scale. All the other parameters were kept fixed.*

The last step is scaling the SNR according to an established number of luminosity distances (d_l). That is possible because, as shown in Figure 3, there is a relationship between the SNR and the luminosity distance (SNR$\propto 1/d_L$). Therefore, a number of luminosity distances are drawn from probability distributions for each of the SNRs calculated in the second step. Then, they are scaled accordingly. The scaling of the SNR using the luminosity distance is a desired operation because it is computationally faster than generating a new waveform for each distance. However, it is important to note that the masses are generated drawing from $p(\vec{\theta}_{det})$, and mass is degenerate with redshift:

$$m_{det} = (1+z)m_{source} \tag{10}$$

Therefore, it is necessary to account for this in the calculation, especially because if we just correct the masses to the correct frame, then the masses of population is not going to follow the mass probability density consistently across redshift. This can be done by drawing the redshift population from a conditional probability distribution:

$$p(z|m_{det}) = \frac{p(z)p(m_{src})}{(1+z)p(m_{det})} \tag{11}$$

It was not possible to conclude the implementation of the correction over the 10-weeks, so the experiments described in this report did not use the luminosity distance scaling.

3 Results

3.1 Calculating the variance of the space-time sensitive hypervolume

As this study uses Monte Carlo simulations to numerically solve for the space-time sensitive hypervolume, it is important to understand how precise the estimations are and how it varies with the size of the population. Therefore, it is necessary to study the variance of the estimated space-time sensitive hypervolume. For this, we varied the number of intrinsic parameters (N): 100, 500, 1000, 5000, and 1000. For each of the N, the $\langle VT \rangle$ was calculated a 1000 times using the bootstrapping method, and histograms were produced to evaluate how precise those results are.

The events were averaged over sky locations, and the population has its source mass of the primary black hole (m_1) drawn from a truncated Gaussian distribution around ($35M_\odot$), with a minimum mass of $25M_\odot$ and a maximum of $35M_\odot$ The spins components of the binary stars are drawn from an uniform distribution.

N	$mean\langle VT \rangle$ (Gpc^3yr)	σ (Gpc^3yr)
100	0.2104	0.0158
500	0.2097	0.0066
1000	0.2095	0.0048
5000	0.2095	0.0021
10000	0.2094	0.0015

Table 1. *The mean $\langle VT \rangle$ and its respective standard deviations calculated for each number N.*

As expected, the results are a Gaussian, and the standard deviation scales proportionally to $1/\sqrt{N}$. For computations, it is always going to be an exchange between precision and run time, as it is possible to use the pipeline for different number of intrinsic parameters depending on the desired precision, but increasing the number of intrinsic parameters increases the run time.

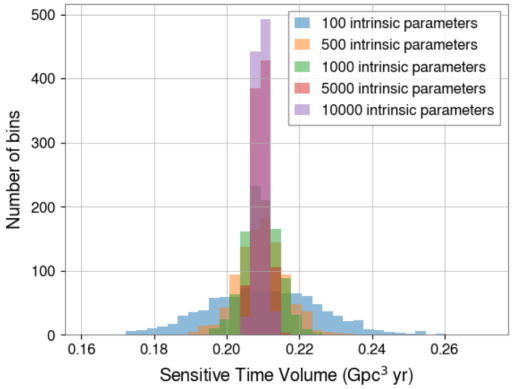

Figure 5. *The space-time sensitive hypervolume distribution, computed over different number of intrinsic parameters.*

3.2 $\langle VT \rangle$ and the spin z component

The second study performed was to determine how the space-time sensitive hypervolume $\langle VT \rangle$ changes according to changes in the aligned spin component. For this, six runs were performed, and for each run the population was drawn from almost the same probability distributions. The only parameter that changed was the aligned spin z of both black holes in the binary system. As for the other parameters, the masses of both black holes (m_1 and m_2) are drawn from a log normal distribution around $\log(35M_\odot)$, and the x and y spins components are set to zero. The computation is averaged over sky positions.

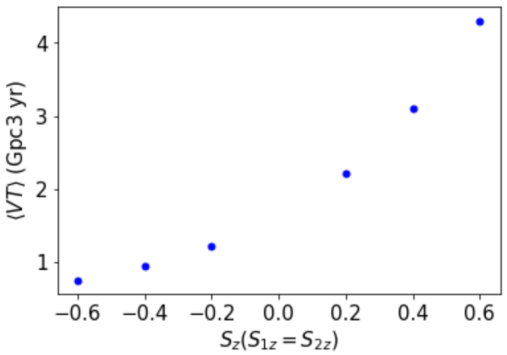

Figure 6. *The space-time sensitive hypervolume calculated for different spin z components. The error bars are smaller than the size of the marker so they can not be seen in this plot.*

In Figure 6, it is possible to observe that the $\langle VT \rangle$ increases with increasing spin. This is exactly what we expected, as the hangup effect predicts that the increase in the aligned spin will increase the length of the inspiral. This will produce a higher SNR, therefore a higher $\langle VT \rangle$.

3.3 $\langle VT \rangle$ and the Higher order modes

The leading order of higher order mode for the gravitational waves is l = m = 2. The IMRPhenomXP is a family of waveform templates [14] that incorporates the inspiral, merger and ring-down stages of the binary black hole coalescence. IMRPhenomXP incorporates the dominant quadrupole spherical harmonic modes, and IMRPhenomXPHM incorporates multipoles beyond the dominant quadrupole in the template waveform [10], including (2, 1), (3, 2), (3, 3), and (4,4).
In this experiment, the objective was to study how the presence of higher order modes in the waveform template affects the $\langle VT \rangle$. For this, a population was generated with both IMRPhenomXP and IMRPhenomXPHM waveforms templates. Then, the $\langle VT \rangle$ was calculated using a combination of different injection and recovery waveforms as shown in Table 1. For this study, population has its masses (m_1 and m_2) drawn from a Delta function distribution around $35M_\odot$.

Further, it has a isotropic spin distribution, and is averaged over sky positions.

Injection	Recovery	$\langle VT \rangle$ Gpc^3yr	σ Gpc^3yr
XPHM	XPHM	1.8509	0.0094
XP	XP	1.8202	0.0096
XPHM	XP	1.6886	0.0092

Table 2. *The injection and recovery waveforms, and the corresponding estimated space-time sensitive hypervolume. XPHM represents IMRPhenomXPHM and XP represents IMRPhenomXP.*

The $\langle VT \rangle$ estimated for the injection and recovery using IMRPhenomXPHM, is greater than the $\langle VT \rangle$ estimated for the injection and recovery using IMRPhenomXP. That is exactly what was expected as the presence of more higher order modes will increase the SNR. For the case where the injection waveform was generated using IMRPhenomXPHM and it was recovered with IMRPhenomXP, the smallest $\langle VT \rangle$ was calculated. That shows that it's harder to detect the signals when the recovery wavefomr template is missing higher order modes.

4 Conclusion

SIFCE is a pipeline capable of efficiently carrying out the $\langle VT \rangle$ calculation, using methods to speed up the calculation, allowing for diverse studies using different population distributions. The experiments conducted produced results that are compatible with the current studies about gravitational waves.
It is possible to conduct numerous experiments with the SIFCE pipeline, including the calculations of the $\langle VT \rangle$ for the next generation of detectors, as well as to study the dependence of $\langle VT \rangle$ in all parameter space. In the future, we plan to continue exploring the parameter space, as well as using more elaborated mass distributions such as the power law plus peak (described in [15])

5 Acknowledgements

I thank Alan Weinstein, Rhiannon Udall, and Jacob Golomb for their tremendous support in this project. I also gratefully acknowledge the support from the National Science Foundation Research Experience for Undergraduates (NSF REU) program, the California Institute of Technology, and the LIGO Summer Undergraduate Research Fellowship.

References

[1] Benjamin P Abbott et al. "Observation of gravitational waves from a binary black hole merger". In: *Physical review letters* 116.6 (2016), p. 061102. DOI: https://doi.org/10.1103/PhysRevLett.116.061102.

[2] Richard Abbott et al. "GWTC-3: compact binary coalescences observed by LIGO and Virgo during the second part of the third observing run". In: *arXiv preprint arXiv:2111.03606* (2021). DOI: https://doi.org/10.48550/arXiv.2111.03606.

[3] Junaid Aasi et al. "Advanced ligo". In: *Classical and quantum gravity* 32.7 (2015), p. 074001. DOI: https://doi.org/10.48550/arXiv.1411.4547.

[4] Bernard Caron et al. "The virgo interferometer". In: *Classical and Quantum Gravity* 14.6 (1997), p. 1461.

[5] "KAGRA: 2.5 generation interferometric gravitational wave detector". In: *Nature Astronomy* 3.1 (2019), pp. 35–40.

[6] Andrew Miller. "Bayesian inference for compact binary coalescences with bilby: validation and application to the first LIGO–Virgo gravitational-wave transient catalogue". In: *Monthly Notices of the Royal Astronomical Society* 499 (2021), p. 3295.

[7] Alex Nitz et al. *gwastro/pycbc*. DOI: 10.5281/zenodo.5347736.

[8] Gregory Ashton et al. "BILBY: A user-friendly Bayesian inference library for gravitational-wave astronomy". In: *The Astrophysical Journal Supplement Series* 241.2 (2019), p. 27.

[9] Benjamin P Abbott et al. "The rate of binary black hole mergers inferred from Advanced LIGO observations surrounding GW150914". In: *The Astrophysical journal letters* 833.1 (2016), p. L1. DOI: https://doi.org/10.48550/arXiv.1602.03842.

[10] Geraint Pratten et al. "Computationally efficient models for the dominant and subdominant harmonic modes of precessing binary black holes". In: *Physical Review D* 103.10 (2021), p. 104056.

[11] Geraint Pratten et al. "Setting the cornerstone for a family of models for gravitational waves from compact binaries: The dominant harmonic for nonprecessing quasicircular black holes". In: *Physical Review D* 102.6 (Sept. 2020). DOI: 10.1103/physrevd.102.064001.

[12] Abhirup Ghosh et al. *Priors*. URL: https://lscsoft.docs.ligo.org/bilby/prior.html.

[13] Richard Udall, Jacob Golomb, and Daniela Yano. *Simple Injection Framework for Computational Estimates (SIFCE)*. https://git.ligo.org/richard.udall/sifce. 2022.

[14] Parameswaran Ajith et al. "Template bank for gravitational waveforms from coalescing binary black holes: Nonspinning binaries". In: *Physical Review D* 77.10 (2008), p. 104017.

[15] The LIGO Scientific Collaboration et al. *The population of merging compact binaries inferred using gravitational waves through GWTC-3*. 2021. DOI: 10.48550/ARXIV.2111.03634.